MUSCLE HISTOLOGY IMAGE ANALYSIS FOR SARCOPENIA: REGISTRATION OF SUCCESSIVE SECTIONS WITH DISTINCT ATPASE ACTIVITY

Olcay Sertel[*†‡], *Belma Dogdas*[‡], *Chi Sung Chiu*[§], *Metin N. Gurcan*[†]

*Dept. of Electrical and Computer Engineering, The Ohio State University, Columbus, OH (USA)
[†]Dept. of Biomedical Informatics, The Ohio State University, Columbus, OH (USA)
[‡]Dept. of Applied Computer Science and Mathematics, Merck & Co., Inc., Rahway, NJ (USA)
[§]Musculo-Skeletal Biology Program Team, Merck & Co., Inc., Boston, MA (USA)

ABSTRACT

One way of evaluating muscle quality is to determine its fiber type composition in histological sections. A complete muscle fiber type characterization system requires combining information from successive muscle histology images with different ATPase stain. Due to the local and global deformations introduced in slide preparation process, a precise non-rigid registration is essential to construct the spatial correspondences between these successive images. This study proposes an approach for automated non-rigid registration of successive muscle histological sections. We propose a feature-based registration that uses a two stage approach: a rigid initialization followed by a non-rigid refinement. The rigid initialization step globally aligns successive tissue slides by finding correspondences between individually segmented muscle fibers using Fourier shape descriptors and computing the global rigid transformation using a voting scheme tolerant to mismatches. In the non-rigid stage we establish precise point correspondences using the normalized cross correlation metric and compute the non-rigid distortion using a polynomial transformation that minimizes the mean square distance between these control points.

Index Terms—histological image registration, muscle fiber typing, sarcopenia.

1. INTRODUCTION

Sarcopenia is the age related loss of skeletal muscle mass, strength and function. As the proportion of elderly people in the population increases, the incidences of sarcopenia are anticipated to increase dramatically [1]. In clinical practice radiological screenings (CT and MRI) and functional performance assays are being used to assess muscle quality; however there is no clearly defined test or an accepted threshold of functional decline for sarcopenia diagnosis [2]. Hence, there is a need for improved methods to measure the muscle quality and better criteria for defining at what level muscle mass and strength become "deficient" [3].

Skeletal muscle consists of individual fibers that are responsible for contraction and force generation. Based on their characteristics with respect to contraction time, force production and resistance to fatigue, muscle fibers are classified as type I, IIA, IIX and IIB [4]. The relative distribution of distinct fiber types in a muscle provides insight into muscle quality. Recent studies showed that there is an association between the loss in type II muscle fibers and sarcopenia [3, 4]. In clinical and laboratory practice, muscle fiber type composition is identified through a qualitative microscopic examination of successive histological cross-sections with distinct ATPase stain. Fig. 1 demonstrates region of interest (ROI) images from two successive serial cross-sections of a rat gastrocnemius muscle stained with ATPase stain at distinct pH levels.

In this study, we propose a registration framework to align serial cross-sections of digitized muscle histology slides for automated muscle fiber characterization. We develop a two-stage approach consisting of a rigid initialization followed by a non-rigid refinement. The rigid initialization globally aligns the tissue slides by finding correspondences between individually segmented muscle fibers from successive slides using their Fourier shape descriptors. The global rigid transformation is computed using a voting scheme tolerant to mismatches. In the non-rigid stage we establish precise point correspondences using the normalized cross correlation metric and compute the non-rigid distortion using a polynomial transformation that minimizes the mean square distance between these control points.

Thanks to Kimberly Pierdolla, Histology Laboratory of the Univ. of Texas Health Science Center, San Antonio, TX (USA), Xianlu Qu and John Reilly, Boston Bioanalytics & Pathology, Merck & Co., Inc., Boston, MA (USA) for their helps during slide preparation and acquisition of muscle histology images and for their support on this work.

[‡]Olcay Sertel performed this work during his internship at Merck & Co., Inc. Rahway, NJ (USA).

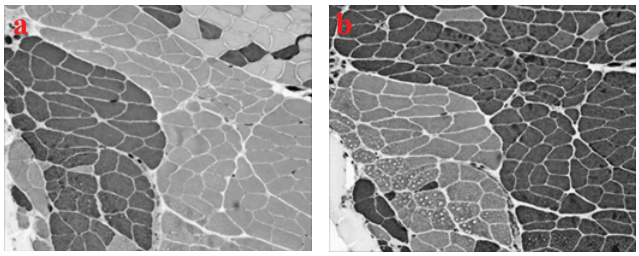

Fig.1 Sample images of successive serial cross-sections of a rat gastrocnemius muscle stained with ATPase at (a) pH 4.5 and (b) 10.4, respectively.

2. METHODS

Image registration is the process of geometrically aligning two images of same or partially overlapping scenes so that the corresponding points in these two images have the same coordinates after transformation [5]. Medical image registration methods, which are reviewed in a number of survey articles [5-7], can be classified according to the nature of registration basis and the nature of transformation. With respect to registration basis, these methods can be classified as feature-based or image content-based methods. According to the nature of transformation, registration methods vary from global rigid, affine and projective to curved transformations, which can be modeled by spline warps or polynomial transformation functions.

Histology applications deal with soft tissue; hence a precise non-rigid registration is essential due to the local and global deformations introduced in the slide preparation process. In [8], authors proposed a hierarchical elastic registration framework using the mutual information metric. As reported in their study, this approach produced acceptable results in only 80% of the cases. Although a mutual information based approach does not assume any functional relationship between the image intensities, it requires the initial positions of the slides (or the region of interest images) to be roughly aligned, otherwise the search space, which maximizes the mutual information metric, is too large and is subject to numerous local minima.

2.1. Data description

In our study, we used frozen histological sections of rat gastrocnemius muscle from young and aged animals (twelve vs. 30 months, respectively). Tissue sections were sectioned at 12μm thickness and were mounted onto glass slides. Successive sections were subjected to acidic and alkaline sensitive ATPase staining at pH levels 4.5 and 10.4, respectively. Finally, tissue slides were imaged with Nikon light microscope at 10x objective and were used for further analysis.

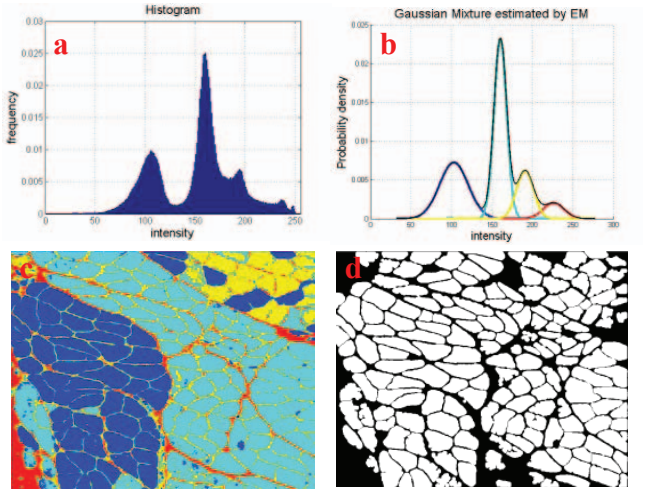

Fig.2 (a) Normalized histogram of the image given in Fig. 1(a), (b) estimated Gaussian mixture model, (c) color labeled segmentation, and (d) segmented muscle fibers.

2.2. Segmentation

The proposed rigid initialization step uses a higher-level context for feature correspondence computation. We first segment individual muscle fibers and calculate their Fourier shape descriptors. These descriptors are used to compute spatial correspondences that are essential to calculate the rigid global transformation.

We use a clustering based approach to segment the muscle histology images. After examining the histograms of the images, we observed that the intensity distribution could be modeled using a Gaussian mixture model, where each component is associated with the intensity distribution of a certain fiber type or the connective tissue surrounding the muscle fibers. The parameters of the mixture (i.e., mean, μ_i and variance, σ_i, where $i = 1, \ldots, n$, and n is the number of mixture components) are estimated using the expectation maximization algorithm [9]. The number of mixture components is also estimated by finding the significant peaks in the image intensity histogram. Finally, we apply morphological operations (e.g., opening, watershed transform) to refine final muscle fiber boundaries. Fig. 2 shows the intermediate steps of the segmentation process for the sample image given in Fig. 1 (a).

2.3. Rigid Initialization

The goal of the rigid initialization step is to globally align the two successive slides so that the search space for the non-rigid refinement is smaller; hence the probability of mismatch is lower leading to a more robust and more precise registration. We propose a feature-based approach, in which we utilize the shape descriptors of the segmented muscle fibers in successive images to compute the correspondences.

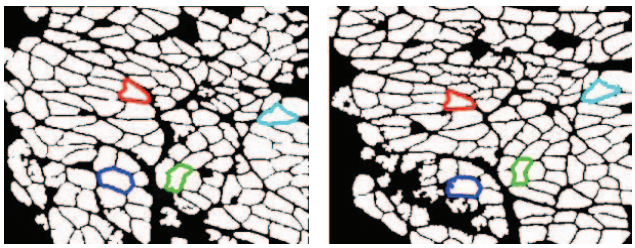

Fig.3 Segmentation of muscle fibers is shown in binary form, while a few of corresponding muscle fibers are shown using the same boundary colors.

We begin by representing the boundary of each fiber as a periodic function in the complex plane:

$$s(t) = x(t) + jy(t) = \sum_{k=-N}^{N} S_k e^{jkt} \text{ for } t \in [0, 2\pi] \quad (2.1)$$

where the complex Fourier descriptors $S_k = a_k + jb_k$, $a_k, b_k \in \Re$ describe the spatial frequency contents of the contour points [10]. Each parameter S_k has a phase, $\phi_k = \tan^{-1}(\frac{b_k}{a_k})$, and a magnitude, $|S_k| = \sqrt{a_k^2 + b_k^2}$. Using Fourier descriptors, we can achieve a compact shape representation invariant to rotation, translation and scale. Rotation only affects the phase component; hence we achieve the rotational invariance by using the magnitude of the complex Fourier descriptors. For translation invariance, we simply discard the S_0 term, which corresponds to the center of mass information. Finally, the scale invariance is achieved by scaling each S_k term by the absolute value of a chosen element (e.g., S_1). Accordingly, the corresponding Fourier shape descriptors are computed as follows:

$$C_{k-2} = |S_k| / |S_1|, \; k = 2,3,\ldots,N-1 \quad (2.2)$$

Using these descriptors, we establish correspondences between muscle fibers in successive images. Fig. 3 shows four sample corresponding muscle fibers in two successive images. In fact, each of the correspondences (i.e., a matching pair of muscle fiber) defines a rigid transformation, which is computed using the iterative closest point (ICP) algorithm [11]. Using the boundary points of the corresponding muscle fibers, the ICP algorithm iteratively computes the rigid registration parameters, i.e., the rotation angle θ, and the translation in x and y directions t_x and t_y, respectively that rigidly aligns the matching pair of muscle fibers.

Ideally, if all the correspondences are correct, the computed values of the rigid transformation parameters for all of the corresponding muscle fiber pairs will be very close to each other. However, there are mismatches in these correspondences due to several reasons (e.g., segmentation inaccuracies, similarly shaped muscle fibers, etc.). In order to compensate these mismatches and to calculate the true global rigid transformation, we use a voting scheme introduced in [12]. Using the rigid transformation parameters computed for all of the corresponding muscle fiber pairs, we construct three histograms for each rigid transformation parameter, θ, t_x and t_y. Our hypothesis is that the correct global transformation corresponds to a peak among all compatible matchings, while the mismatches generate random transformations in the entire solution space. Fig. 4 shows the histograms of the rigid transformation parameters θ, t_x, and t_y, constructed for the sample successive ROI images.

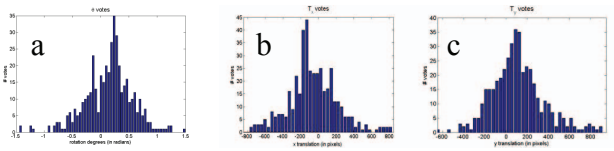

Fig.4 Sample histogram voting results for rigid initialization parameters (a) θ, (b) tx, and (c) ty, where peaks locations correspond to the resulting global rigid alignment.

2.4. Non-rigid refinement

Due to the non-rigid deformations introduced during the slide preparation process, there are local misalignments between the two images after the global rigid initialization stage. In the non-rigid registration stage, we use a set of control points (i.e., sub-sampled muscle fiber boundary points) that are fairly distributed in the spatial domain. In order to precisely localize the corresponding matching location in both images, we use a small patch (e.g., 32×32) around these candidate control points and generate the normalized cross correlation (NCC) surface over a slightly larger window (e.g., 64×64) around the corresponding location determined using the rigid initialization in the successive image. The NCC is robust to intensity variations between distinctly stained images; hence it can capture the structural similarities and allow us to compute precise point correspondences [7]. For each control point, we update the correct match location using the offset associated with the peak in the resulting NCC surface.

Among commonly used non-rigid transformations such as thin-plate spline, local weighted mean or polynomial, we choose polynomial transformation. Compared to others, polynomial transformation is faster to compute and it provides satisfactory results in correcting the distortions encountered in our histological sections. In our application, we use second degree polynomials. For a set of N control point pairs (x_i, y_i) and (x_i', y_i'), the second degree polynomial transformation is expressed as follows:

$$\begin{cases} x_i' = a_1 x_i^2 + b_1 x_i y_i + c_1 y_i^2 + d_1 x_i + e_1 y_i + f_1 \\ y_i' = a_2 x_i^2 + b_2 x_i y_i + c_2 y_i^2 + d_2 x_i + e_2 y_i + f_2 \end{cases} \quad (2.3)$$

where $i = 1,2,\ldots,N$ and $a,\ldots,f$ are the coefficients of the polynomial transformation, which are computed using least squares minimization.

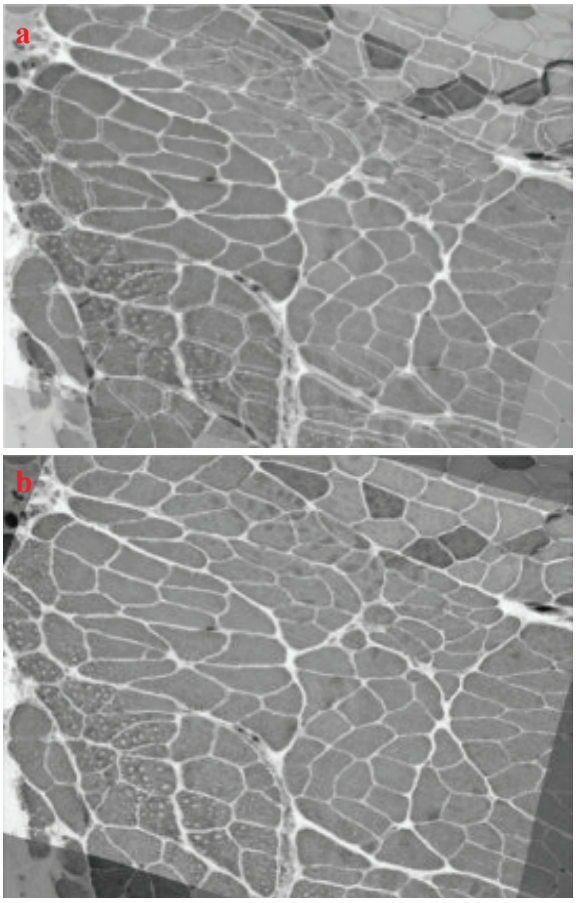

Fig.5 Sample successive region of interest images are overlaid together after (a) global rigid initialization, and (b) non-rigid refinement.

3. EXPERIMENTAL RESULTS

Fig. 5 shows the registration results for the sample ROIs from successive tissue regions by overlaying the two images after global rigid initialization and non-rigid refinement stages. Although the center regions in the image are well-aligned (see Fig. 5 (a)), there are misalignments in the upper right and lower regions. Fig. 5 (b) shows the two images overlaid after the non-rigid refinement stage, which corrects such local deformations and aligns the two images accurately.

We applied the proposed registration framework on six pair -three from young and three from aged rats- of ROI images captured from successive muscle tissue slides stained with ATPase stain at pH=4.5 and pH=10.4. Motivated by our goal of muscle fiber typing, we evaluated the proposed registration approach by comparing the overlap score between individual muscle fibers manually marked in successive images. For practical reasons, we manually delineated five muscle fibers in each pair of successive images and computed the overlap ratio as follows:

$$s = \frac{Area(F_{pH=4.5} \cap T(F_{pH=10.4}))}{\max(Area(F_{pH=4.5}), Area(F_{pH=10.4}))} \qquad (3.1)$$

where $F_{pH=4.5}$ and $F_{pH=10.4}$ are the muscle fibers delineated in successive images with different ATPase stain, and T is the computed transformation matrix between the two images. Using this overlap measure, the proposed registration approach produced a remarkable overlap score of 94.5±3.2%, which is promising for future applications.

4. SUMMARY

This study presents a registration approach to spatially align distinctly stained muscle histology slides for automated muscle fiber characterization. Using high-level shape features, we first compute the rigid initialization. The non-rigid refinement is achieved by establishing precise point correspondences using the NCC metric. Validation over a set of image pairs demonstrates promising results for future applications.

5. REFERENCES

[1] G. S. Lynch, J. D. Schertzer and J. G. Ryall, Therapeutic approaches for muscle wasting disorders, *Pharmacology and Therapeutics*, 113, pp. 461-487, 2007.

[2] L. J. S. Greenlund and K. S. Nair, Sarcopenia—consequences, mechanisms, and potential therapies *Mechanisms of Ageing and Development*, 124(3), pp. 287-299, 2003.

[3] J. E. Morley, R. N. Baumgartner, R. Roubenoff, J. Mayer and K. S. Nair, Sarcopenia, *Journal of Laboratory and Clinical Medicine*, 137(4), pp. 231-243, 2001.

[4] A. Briguet, I. Courdier-Fruh, M. Foster, T. Meier and J. P. Magyar, Histological parameters for the quantitative assessment of muscular dystrophy in the mdx-mouse, *Neuromuscular Disorders*, 14, pp. 675-682, 2004.

[5] D. L. Hill, P. G. Batchelor, M. Holden and D. J. Hawkes, Medical image registration, *Physics in Medicine and Biology*, 46, pp. 1-45, 2001.

[6] J. B. Maintz and M. A. Viergever, A survey of medical image registration *Medical Image Analysis*, 2(1), pp. 1-36, 1998.

[7] B. Zitova and J. Flusser, Image registration methods: A survey, *Image and Vision Computing*, 21, pp. 977-1000, 2003.

[8] B. Likar and F. Pernus, Registration of serial transverse sections of muscle fibers, *Cytometry*, 37, pp. 93-106, 1999.

[9] R. O. Duda, P. E. Hart and D. G. Stork, Pattern classification, Wiley-Interscience, 2001.

[10] M. Sonka, V. Hlavac and R. Boyle, Image processing, analysis, and machine vision Chapman & Hall Computing, 1998.

[11] Z. Zhang, Iterative point matching for registration of free-form curves and surfaces, *Int. Journal of Computer Vision*, 13(2), pp. 119-152, 1992.

[12] K. Huang, L. Cooper, A. Sharma and T. Pan, Fast automatic registration algorithm for large microscopy images, *IEEENLM Life Science Systems & Applications Workshop*, pp. 1-2, 2006.